

Dynamical fragile topology in Floquet crystalsJiabin Yu^{1,*}, Yang Ge,² and Sankar Das Sarma¹¹*Condensed Matter Theory Center and Joint Quantum Institute, Department of Physics, University of Maryland, College Park, Maryland 20742, USA*²*Department of Physics, University of Cincinnati, Cincinnati, Ohio 45221, USA*

(Received 30 March 2021; accepted 25 October 2021; published 9 November 2021)

Although fragile topology has been intensely studied in static crystals in terms of Wannier obstruction, it is not clear how to generalize the concept to dynamical systems. In this work we generalize the concept of fragile topology, and provide a definition of fragile topology for noninteracting Floquet crystals, which we refer to as dynamical fragile topology. In contrast to the static fragile topology defined by Wannier obstruction, dynamical fragile topology is defined for the nontrivial quantum dynamics characterized by the obstruction to static limits (OTSL). Specifically, the OTSL of a Floquet crystal is fragile if and only if it disappears after adding a symmetry-preserving static Hamiltonian in a direct-sum way preserving the relevant gaps (RGs). We further present a concrete 2 + 1D example for dynamical fragile topology, based on a model that is qualitatively the same as the dynamical model with anomalous chiral edge modes in Rudner *et al.* [*Phys. Rev. X* **3**, 031005 (2013)]. The fragile OTSL in the 2 + 1D example exhibits anomalous chiral edge modes for a natural open boundary condition, and does not require any crystalline symmetries besides lattice translations. Our work paves the way to study fragile topology for general quantum dynamics.

DOI: [10.1103/PhysRevB.104.L180303](https://doi.org/10.1103/PhysRevB.104.L180303)**I. INTRODUCTION**

In static band insulators, nontrivial topology [1–3] is defined by Wannier obstruction [4–7], i.e., obstruction to the existence of maximally localized symmetric Wannier functions for the ground state. Here maximally localized symmetric Wannier functions can be intuitively viewed as localized atomic orbitals. Continuously deforming a topological insulator (by definition having Wannier obstruction) into an atomic insulator (by definition having no Wannier obstruction) must either break certain symmetries or close the gap near the Fermi energy. Wannier obstruction of a topological insulator is defined to be fragile [8,9] if the obstruction disappears after adding an atomic limit to the occupied subspace in a symmetry-preserving way [Fig. 1(a)]. The K-theoretic classification, as well as the corresponding bulk-boundary correspondence, of stable topology [1–3,10,11] fails to fully capture fragile topology, since K theory [12] requires a stable equivalence which is immune to adding trivial systems. Therefore, considerable research efforts [8,9,13–35] have been dedicated to characterizing and understanding fragile topology during the last three years. In particular, nontrivial boundary signatures of eigenvalue-indicated fragile phases have been experimentally observed in an acoustic metamaterial with a specially constructed twisted boundary condition [22,23]. However, it is not straightforward to impose such a twisted boundary condition on naturally occurring condensed matter systems, such as twisted bilayer graphene, which has been predicted to host fragile topology [17,36–45] (unless

the emergent particle-hole symmetry is strictly imposed [42]). Nontrivial [46] boundary signatures of fragile topology for natural open boundary conditions remain elusive [25]. Furthermore, all the examples of fragile topology previously studied require crystalline symmetries in addition to lattice translations.

An important open question is how to generalize the concept of fragile topology from static crystals to dynamical systems. A classic type of dynamical systems are noninteracting Floquet systems—noninteracting systems with time-periodic Hamiltonians—which is the focus of this work. In recent years, the topology in Floquet systems has been intensely studied [47–78], especially in the presence of crystalline symmetries [79–104]. In particular, Ref. [98] discussed the fragility of Wannier obstruction in Floquet crystals. However, nontrivial dynamics of Floquet crystals is characterized by OTSL instead of Wannier obstruction [55,62,64,67,69–72,78,103]. Only Floquet crystals with OTSL can exhibit phenomena that are forbidden in static crystals, such as anomalous chiral edge modes [55] in the absence of nonzero Chern numbers [105]. Then, the specific question that we will address is whether the concept of fragile topology can be naturally generalized to the dynamical setting of Floquet crystals with OTSL, regardless of static Wannier obstruction.

In this work we provide a natural definition of fragile topology with respect to OTSL [Fig. 1(b)], which we refer to as dynamical fragile topology. Specifically, the OTSL of a topologically nontrivial Floquet crystal is fragile if and only if the OTSL disappears after adding a symmetry-preserving static Hamiltonian in a direct-sum way that preserves RGs. Here the precisely defined RGs are topologically relevant quasienergy band gaps, as explained later. By definition, dynamical fragile

*jiabinyu@umd.edu

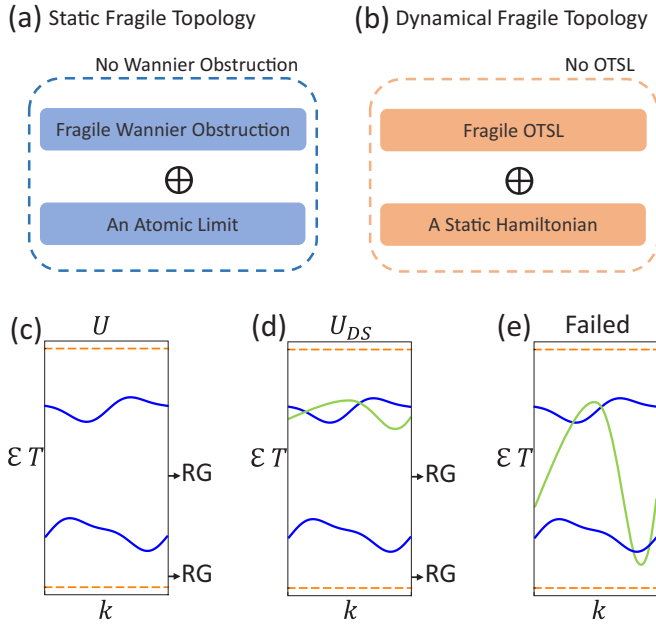


FIG. 1. In (a) and (b) we schematically show the definitions of static fragile topology and dynamical fragile topology. In (c) we schematically plot the quasienergy bands for a two-band 1 + 1D Floquet crystal U , for which we choose both quasienergy gaps to be RGs. In either (d) or (e) we schematically plot the quasienergy bands of a direct-sum system that consists of U (blue) and an added one-band static Hamiltonian (green). In (d) both RGs of U are preserved, while one RG of U is closed in (e). In (c)–(e) all quasienergy bands are plotted in a time-independent phase Brillouin zone (PBZ) $[\Phi_k, \Phi_k + 2\pi)$ with the PBZ lower bound Φ_k in a RG (if RGs exist). The orange dashed lines mark the boundaries of the PBZ.

topology cannot be fully captured by K-theory as long as static limits (i.e., Floquet crystals with static Hamiltonians) are treated as trivial systems. To demonstrate the existence of dynamical fragile topology in tight-binding models, we provide a concrete 2 + 1D example that has no crystalline symmetries besides lattice translations, based on a slight modification of the model in Ref. [55]. In particular, the 2 + 1D example has anomalous chiral edge modes for a natural open boundary condition. Therefore, unlike static fragile topology, dynamical fragile topology does not rely on crystalline symmetries besides lattice translations, and can have nontrivial boundary signatures for natural open boundary conditions.

II. GENERAL DISCUSSION

A noninteracting Floquet system can be described by a time-periodic single-particle Hamiltonian $H(t) = H(t + T)$ with $T > 0$ the time period, and the corresponding time-evolution operator given by the Dyson series reads

$$U(t) = \mathcal{T} \exp \left[-i \int_0^t dt' H(t') \right] \quad (1)$$

satisfying $U(t + T) = U(t)U(T)$. In Eq. (1), \mathcal{T} is the time-ordering operator, $\hbar = 1$ is chosen, and the initial time is set to zero without loss of generality [103].

Time-reversal symmetry of $H(t)$ can be naturally broken by the dynamics, and crystals in normal phases typically do

not have particle-hole or chiral symmetries; thus we can focus on symmetry class A [71] in which time-reversal, particle-hole, and chiral symmetries are all absent. Nevertheless, $H(t)$ can preserve a time-independent crystalline symmetry group \mathcal{G} . Examples of \mathcal{G} include space groups in 3 + 1D and plane groups in 2 + 1D, which may contain lattice translation symmetries, rotation symmetries, mirror symmetries, and so on. The lattice translation symmetries in \mathcal{G} allow us to label the time-independent bases of the underlying single-particle Hilbert space as $|\psi_{k,a}\rangle$, where \mathbf{k} is a Bloch momentum in the first Brillouin zone (1BZ), and a takes N different values for all other degrees of freedom (e.g., spin and orbital). By defining $|\psi_{\mathbf{k}}\rangle = (\cdots |\psi_{k,a}\rangle \cdots)$, $H(t)$ and $U(t)$ in the space spanned by $|\psi_{\mathbf{k}}\rangle$ are represented as

$$H(t) = \sum_{\mathbf{k}} |\psi_{\mathbf{k}}\rangle h(\mathbf{k}, t) \langle \psi_{\mathbf{k}}|, \quad U(t) = \sum_{\mathbf{k}} |\psi_{\mathbf{k}}\rangle U(\mathbf{k}, t) \langle \psi_{\mathbf{k}}|. \quad (2)$$

Eigenvalues of $U(\mathbf{k}, T)$ have the form $e^{-i\epsilon_{m,\mathbf{k}}T}$ with $m = 1, \dots, N$, and $\epsilon_{m,\mathbf{k}}$ are called quasienergy bands.

The quasienergy band gaps play a particularly important role in Floquet topology [62,71,72,103], similar to that of energy band gaps in static band topology. Nevertheless, unlike a static band insulator whose physically relevant band gap is uniquely determined by the filling, Floquet systems like U do not have a well-defined occupied subspace, and thereby we have to choose relevant quasienergy band gaps (i.e., RGs) for them based on the physics of interest. In other words, choice of RGs is an essential step in describing Floquet topology. After choosing RGs for U , we arrive at a Floquet crystal U that is characterized by its time-evolution operator $U(t)$ equipped with the time period T , the RG choice, and the crystalline symmetry group \mathcal{G} . [See Fig. 1(c) for a schematic example].

According to Refs. [62,103] the topological equivalence between two \mathcal{G} -invariant Floquet crystals is defined by a continuous deformation that connects them while preserving \mathcal{G} and all RGs. Then, as proposed in Ref. [103], a Floquet crystal is defined to have OTSL if and only if it is topologically distinct from all \mathcal{G} -invariant static limits [106]. In other words, given a Floquet crystal U with \mathcal{G} , it has OTSL if and only if we cannot continuously deform U into the time-evolution operator of any static Hamiltonian while preserving all symmetries in \mathcal{G} and keeping open all RGs of U . For example, the 2 + 1D two-band dynamical model in Ref. [55], which has zero Chern numbers and has anomalous chiral edge modes, has OTSL if all bulk quasienergy gaps are chosen to be RGs. The reason is that 2 + 1D static systems cannot have chiral edge modes when all bands have zero Chern numbers, and thus connecting the 2 + 1D dynamical model to any 2 + 1D static crystal in a symmetry-preserving way must close certain RGs to change the Chern numbers. For general 2 + 1D Floquet systems with \mathcal{G} containing only lattice translation symmetries, Refs. [55,62,71] suggests to classify them by a winding number W defined in Ref. [55] and the Chern numbers of the bulk quasienergy bands. Based on Ref. [55], a nonzero W and zero Chern numbers can indicate OTSL when all bulk quasienergy gaps are relevant, since a nonzero W in this case can indicate the existence of anomalous chiral edge modes. But a nonzero W itself does not necessarily indicate

OTSL, since static systems can have nonzero W 's as Ref. [55] pointed out. One experimental signature of OTSL (though not conclusive) is the closing of certain RGs when deforming the dynamical system to any static limit while preserving \mathcal{G} . We believe this signature of OTSL is experimentally accessible since tracking the quasienergy spectrum while deforming the systems has been achieved in experiments like Ref. [78].

We now define dynamical fragile topology [Fig. 1(b)]. Suppose the Floquet crystal U has OTSL. Its OTSL is defined to be fragile if and only if the OTSL disappears after adding a \mathcal{G} -invariant static Hamiltonian H_{SL} in a direct-sum way that preserves all RGs. H_{SL} is allowed to have additional symmetries that are absent in the Floquet crystal U , but they are irrelevant to our discussion. The direct-sum way is required by K-theory, suggesting that the bases of H_{SL} , denoted by $|\psi_{\mathbf{k}}^{\text{SL}}\rangle = (\cdots |\psi_{\mathbf{k},a_{\text{SL}}}^{\text{SL}}\rangle \cdots)$, must be orthogonal to the bases $|\psi_{\mathbf{k},a}\rangle$ of U . Then the underlying Hilbert space of the direct-sum Hamiltonian $H_{\text{DS}}(t) = H(t) + H_{\text{SL}}$ is spanned by $|\psi_{\mathbf{k}}^{\text{DS}}\rangle = (|\psi_{\mathbf{k}}\rangle, |\psi_{\mathbf{k}}^{\text{SL}}\rangle)$. In this direct-sum space, the time-evolution operator $U_{\text{DS}}(t)$ is represented as

$$U_{\text{DS}}(t) = \sum_{\mathbf{k}} |\psi_{\mathbf{k}}^{\text{DS}}\rangle U_{\text{DS}}(\mathbf{k}, t) \langle \psi_{\mathbf{k}}^{\text{DS}}|, \quad (3)$$

where

$$U_{\text{DS}}(\mathbf{k}, t) = \begin{pmatrix} U(\mathbf{k}, t) & \\ & e^{-ih_{\text{SL}}(\mathbf{k})t} \end{pmatrix}, \quad (4)$$

and $h_{\text{SL}}(\mathbf{k})$ is the continuous representation of H_{SL} furnished by $|\psi_{\mathbf{k}}^{\text{SL}}\rangle$. Since H_{SL} is \mathcal{G} invariant, $U_{\text{DS}}(t)$ also preserves \mathcal{G} .

Preserving RGs means that all RGs of U are kept open in the quasienergy band structure given by $U_{\text{DS}}(\mathbf{k}, T)$. [See a RG-preserving example U_{DS} in Fig. 1(d) and nonpreserving example in Fig. 1(e).] Then we can choose the RGs of U_{DS} to be the same as those of U . Combined with the time period T and the crystalline symmetry group \mathcal{G} , we now have a direct-sum Floquet crystal U_{DS} . The absence of OTSL in turn means that U_{DS} has no OTSL, or equivalently $U_{\text{DS}}(t)$ can be continuously deformed into the time-evolution operator of a static Hamiltonian without breaking symmetries in \mathcal{G} and without closing any RGs of U_{DS} . Although there is no off-diagonal coupling in Eq. (4), symmetry-preserving couplings are allowed when constructing the deformation of U_{DS} . Crucially, as long as we can find one H_{SL} that yields a direct-sum U_{DS} without OTSL, the OTSL of U is fragile.

We emphasize that any fragile OTSL that satisfies the above definition is still fragile even if we allow U_{DS} to close RGs of U . The intuition is that if U_{DS} closes certain RGs of U [like Fig. 1(e)] and we choose the remaining RGs of U as RGs of U_{DS} , it would be easier for U_{DS} to lose OTSL since the deformation of U_{DS} is constrained by fewer RGs. Furthermore, our general discussion does not rely on specific RG choices for the dynamical U . One straightforward RG choice for the dynamical U is taking all quasienergy gaps to be relevant, which has been adopted in both theoretical [62] and experimental [78] works, while other choices are also consistent with the above definition. In general, there are no efficient methods of determining fragile OTSL, because there is no rigorously proven complete topological classification for generic Floquet crystals with arbitrary crystalline symmetry groups. In other words, even if the direct-sum U_{DS}

TABLE I. The nonzero expressions of $d_{x,y}$ in the Hamiltonian in Eq. (5) within one time period. $d_{x,y} = 0$ for $t \in [0, \frac{T}{5}) \cup [\frac{4T}{5}, T)$.

t	$[\frac{T}{5}, \frac{2T}{5})$	$[\frac{2T}{5}, \frac{3T}{5})$	$[\frac{3T}{5}, \frac{4T}{5})$
d_x	$-1.25 \cos(k_y)$	$-1.25 \cos(k_x - k_y)$	$-1.25 \cos(k_x)$
d_y	$1.25 \sin(k_y)$	$-1.25 \sin(k_x - k_y)$	$-1.25 \sin(k_x)$

has trivial topological invariants according to the currently known classification, there is no proof that U_{DS} must have no OTSL. Therefore, we cannot tell from the known classification whether fragile OTSL exists in tight-binding models. In order to prove the existence, we present below a concrete example demonstrating fragile OTSLs.

III. 2 + 1D EXAMPLE WITH $p1$ PLANE GROUP

Based on a slightly modified version of the model in Ref. [55], we introduce a 2 + 1D example that has fragile OTSL. In particular, we will demonstrate that dynamical fragile topology can have nontrivial boundary signatures for a natural open boundary condition. The crystalline symmetry group for this example is $\mathcal{G} = p1$, which only contains lattice translations. For the dynamical model, we consider a square lattice with two spinless localized orbitals (labeled by 1,2) on each lattice site, resulting in the bases $|\psi_{\mathbf{k}}\rangle = (|\psi_{\mathbf{k},1}\rangle, |\psi_{\mathbf{k},2}\rangle)$. With these bases, the two-band tight-binding Hamiltonian $H(t)$ that we use is represented as

$$h(\mathbf{k}, t) = E_0 \sigma_0 + d_x(\mathbf{k}, t) \sigma_x + d_y(\mathbf{k}, t) \sigma_y + \delta \sigma_z, \quad (5)$$

where $h(\mathbf{k}, t + T) = h(\mathbf{k}, t)$ with $T = 2\pi$ determining the unit of energy, the lattice constant is set as the unit of length, $E_0 = 0.01$, $\delta = 0.1$, and the detailed expressions of d_x and d_y are shown in Table I.

The time-evolution operator $U(t)$ and time-evolution matrix $U(\mathbf{k}, t)$ in the space spanned by $|\psi_{\mathbf{k}}\rangle$ can be derived from Eqs. (1) and (2). We plot the bulk quasienergy bands of the dynamical U in Fig. 2(a), showing two bulk quasienergy bands and two bulk quasienergy gaps. By choosing both bulk quasienergy gaps to be RGs, we complete a Floquet crystal U with time period T and $\mathcal{G} = p1$. Direct calculation shows that each bulk quasienergy band has a zero Chern number. We further plot the quasienergy bands of U for an open boundary condition along y in Fig. 2(b), which shows one chiral gapless mode in each bulk RG at each edge. According to Ref. [55], such chiral edge modes are anomalous, and U must have OTSL, because chiral edge modes are forbidden in static systems with only vanishing Chern numbers [106]. We emphasize that the model Eq. (5) is qualitatively the same as the dynamical two-band model with anomalous edge modes in Ref. [55], since (i) both models have two bulk quasienergy bands with zero Chern numbers, (ii) both models have one anomalous chiral edge mode at each edge in each bulk quasienergy gap, and (iii) both models have the winding number W defined in Ref. [55] being 1 [106]. The explicit differences between them, which are minor, are detailed in [106].

Next we show that the OTSL of U is fragile. To do so, we need to add a static Hamiltonian to form a direct-sum Floquet crystal. The static Hamiltonian that we add is a two-band static

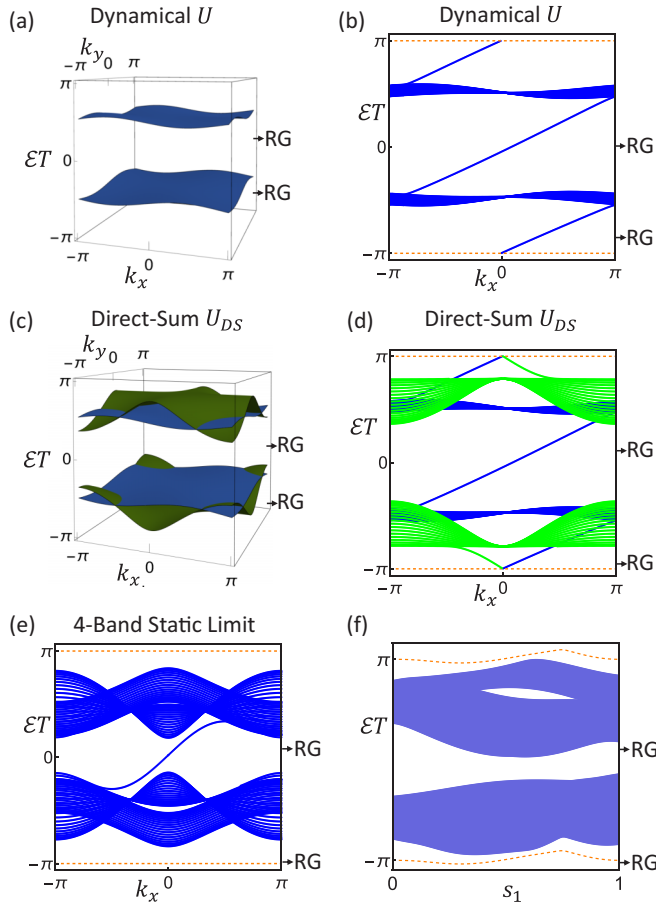


FIG. 2. In this figure we show the dynamical fragile topology in the 2 + 1D example. All RGs are labeled according to the bulk quasienergy bands. In (a) and (c) we plot the bulk quasienergy bands of dynamical U and direct-sum U_{DS} , respectively, in the PBZ $[-\pi, \pi)$. In (b), (d), and (e) we plot quasienergy bands of the dynamical U , the direct-sum U_{DS} , and a four-band static limit, respectively, for an open boundary condition along y . Specifically, we choose 20 lattice sites along y , and only include bulk states (dense lines) and the $(0\bar{1})$ -edge states (in-gap isolated lines) for (b), (d), and (e). The orange dashed lines are the PBZ boundaries. In (c) and (d) the quasienergy bands given by the dynamical U and the added static Hamiltonian H_{SL} are, respectively, marked in blue and green. In (f) we show the quasienergy range (purple regions) of bulk quasienergy bands derived from the deformation $\tilde{U}_{2D,s_1}(T)$. The white regions indicate the deformed RGs, and the orange dashed lines are the deformed PBZ boundaries.

tight-binding Hamiltonian H_{SL} on the same square lattice as the dynamical U . We consider two localized orbitals (labeled as 3,4) on each lattice site for H_{SL} , and make sure that the resultant bases $|\psi_k^{SL}\rangle = (|\psi_{k,3}\rangle, |\psi_{k,4}\rangle)$ are orthogonal to the bases of the dynamical U . We choose the matrix representation of H_{SL} as

$$h_{SL}(\mathbf{k}) = \frac{1}{2} + \frac{1}{3\pi} [M(\mathbf{k})\sigma_z + \sin(k_x)\sigma_x + \sin(k_y)\sigma_y], \quad (6)$$

where $M(\mathbf{k}) = \cos(k_x) + \cos(k_y) - 1$, and $h_{SL}(\mathbf{k})$ represents a simple lattice model for the quantum anomalous Hall effect [107]. Quantum anomalous Hall effect has been experimen-

tally realized [108,109]. According to Eq. (3), the bases of the direct-sum Hamiltonian $H_{DS}(t) = H(t) + H_{SL}$ are $|\psi_k^{DS}\rangle = (|\psi_k\rangle, |\psi_k^{SL}\rangle)$, and the matrix representation $U_{DS}(\mathbf{k}, t)$ of the time-evolution operator $U_{DS}(t)$ can be derived by Eq. (4). As shown in Fig. 2(c), the four bulk quasienergy bands given by $U_{DS}(\mathbf{k}, T)$ keep open both bulk RGs of U . We can then choose the bulk RGs of U to be the RGs of U_{DS} , giving us a direct-sum Floquet crystal U_{DS} together with T and $\mathcal{G} = p1$.

In particular, the bulk bands of the static Hamiltonian H_{SL} have nonzero Chern numbers, which give one chiral edge mode on each edge [Fig. 2(d)]. The chiral edge mode brought by H_{SL} crosses with a counterpropagating chiral edge mode of the dynamical U in the lower bulk RG. As the crossing is unstable, the structure of the chiral modes suggests that the direct-sum U_{DS} might be topologically equivalent to a four-band static limit shown in Fig. 2(e). To confirm it, we construct a continuous deformation $\tilde{U}_{2D,s_1}(t)$ from U_{DS} ($s_1 = 0$) to the four-band static limit ($s_1 = 1$). As shown in Fig. 2(f), both RGs of U_{DS} are kept open along the deformation ($s_1 \in [0, 1)$) and become the RGs of the four-band static limit at $s_1 = 1$, indicating that U_{DS} is topologically equivalent to the four-band static limit and thus has no OTSL [106]. Therefore, OTSL of the dynamical U is fragile, and the fragile OTSL has anomalous chiral edge modes for a natural open boundary condition. Moreover, the fragile OTSL does not need any crystalline symmetries besides lattice translations.

IV. PHYSICAL IMPLICATIONS

We now discuss the physical implications of the defined dynamical fragile topology. One way [48,57,110,111] to generate a well-defined Floquet system is applying a temporal drive to certain modes in a static system, while leaving the other modes (effectively) static. For example, Ref. [57] used laser to excite only the low-energy electrons in a sample, leaving high-energy modes (effectively) undriven. For this method, it is important to carefully control the applied drive (like carefully choosing the laser wavelength in the above example [57]) so that the driven modes have negligible coupling to the remaining static modes. Then, the driven modes form an isolated Floquet subsystem, which can have well-defined OTSL.

One natural question is whether the OTSL in such a Floquet subsystem still exists if the coupling between the subsystem and the surrounding static modes becomes strong. Our definition provides a formalism to address this question. Specifically, when the dynamical U is a Floquet subsystem with OTSL, the added static Hamiltonian H_{SL} will correspond to the surrounding static modes that might have large coupling to U . In a physical situation where the coupling between U and the surrounding static modes is allowed to be nonzero, the nonzero coupling may introduce nonzero off-diagonal coupling in Eq. (4). Then, the OTSL of the entire system should be determined by the direct-sum U_{DS} rather than U , since U is not isolated and the nonzero off-diagonal coupling in Eq. (4) can be naturally included during the deformation of U_{DS} . In this case, if U_{DS} has no OTSL, it means that the OTSL in U can be destroyed by the surrounding static modes, and thereby is fragile. In other words, if the Floquet subsystem

U has fragile OTSL, its OTSL will disappear when certain surrounding static modes are included.

Even if the dynamical U is not a subsystem of a larger system, it is also possible to test the fragility of OTSL in U by explicitly adding a static Hamiltonian. For example, the $2 + 1D$ Floquet topological phases with anomalous edge modes have been observed in a cold-atom system [78] and a photonic system [69]. In the photonic waveguide arrays, the fragility of OTSL may be tested by adding a set of straight waveguides as a static Hamiltonian [59,112].

V. CONCLUSION AND DISCUSSION

To sum up, we introduce a definition for dynamical fragile topology with respect to OTSL, and present a concrete $2 + 1D$ example. The $2 + 1D$ example shows that dynamical fragile topology does not rely on crystalline symmetries other than just lattice translations, and can have clear boundary signatures—such as anomalous chiral edge modes—for a natural open boundary condition.

In the presence of crystalline symmetries beyond lattice translations, dynamical fragile topology can also exist in tight-binding models. To demonstrate this point, we construct a $1 + 1D$ model with inversion symmetry, which is carefully discussed in Ref. [106]. Briefly speaking, the $1 + 1D$ dynamical model with OTSL is given by a chain of spinless s and p orbitals with time-dependent onsite energy and nearest-neighbor hopping, and its OTSL disappears after adding a static chain of spinless d orbitals. This example also shows that the fragile OTSL in certain cases can be destroyed by adding a static atomic insulator. We emphasize that although

we destroyed the fragile OTSL in the $2 + 1D$ example by adding a Chern insulator, we cannot rule out the possibility that adding certain static atomic insulators may also do the job. Finding such static atomic insulators for the $2 + 1D$ example would be an interesting future direction. Furthermore, although our work focuses on symmetry class A, the definition of dynamical fragile topology can be generalized to other symmetry classes by including more internal symmetries.

Finally, we compare and contrast our results to Ref. [71]. Reference [71] presented a K-theoretic classification of unitary loops (i.e., time-periodic unitary evolution) of Floquet crystals. We emphasize that Ref. [71] defined dynamical topological systems by nontrivial unitary loops, while we use the OTSL definition proposed in Ref. [103]. Having nontrivial unitary loops is not equivalent to having OTSL, because static limits may have nontrivial unitary loops. (See Appendix A of this work and Appendix C of Ref. [55].) Due to the different definitions, the dynamical model in the $2 + 1D$ example is identified as stable dynamical topological by the K-theoretic classification in Ref. [71], while we find a fragile OTSL in it [106].

ACKNOWLEDGMENTS

J. Yu thanks Yu-An Chen, Biao Lian, Zhi-Da Song, Xiao-Qi Sun, Zhi-Cheng Yang, and Rui-Xing Zhang for helpful discussions. In particular, J. Yu thanks Zhi-Da Song for providing critical comments, and thanks Xiao-Qi Sun for the information on straight waveguides as static Hamiltonians in photonic systems. This work is supported by the Laboratory for Physical Sciences.

-
- [1] M. Z. Hasan and C. L. Kane, Colloquium: Topological insulators, *Rev. Mod. Phys.* **82**, 3045 (2010).
 - [2] X.-L. Qi and S.-C. Zhang, Topological insulators and superconductors, *Rev. Mod. Phys.* **83**, 1057 (2011).
 - [3] C.-K. Chiu, J. C. Y. Teo, A. P. Schnyder, and S. Ryu, Classification of topological quantum matter with symmetries, *Rev. Mod. Phys.* **88**, 035005 (2016).
 - [4] A. A. Soluyanov and D. Vanderbilt, Wannier representation of \mathbb{Z}_2 topological insulators, *Phys. Rev. B* **83**, 035108 (2011).
 - [5] B. Bradlyn, L. Elcoro, J. Cano, M. Vergniory, Z. Wang, C. Felser, M. Aroyo, and B. A. Bernevig, Topological quantum chemistry, *Nature (London)* **547**, 298 (2017).
 - [6] H. C. Po, A. Vishwanath, and H. Watanabe, Symmetry-based indicators of band topology in the 230 space groups, *Nat. Commun.* **8**, 50 (2017).
 - [7] J. Kruthoff, J. de Boer, J. van Wezel, C. L. Kane, and R.-J. Slager, Topological Classification of Crystalline Insulators through Band Structure Combinatorics, *Phys. Rev. X* **7**, 041069 (2017).
 - [8] H. C. Po, H. Watanabe, and A. Vishwanath, Fragile Topology and Wannier Obstructions, *Phys. Rev. Lett.* **121**, 126402 (2018).
 - [9] J. Cano, B. Bradlyn, Z. Wang, L. Elcoro, M. G. Vergniory, C. Felser, M. I. Aroyo, and B. A. Bernevig, Topology of Disconnected Elementary Band Representations, *Phys. Rev. Lett.* **120**, 266401 (2018).
 - [10] A. Kitaev, Periodic table for topological insulators and superconductors, *AIP Conf. Proc.* **1134**, 22 (2009).
 - [11] D. S. Freed and G. W. Moore, Twisted equivariant matter, *Ann. Henri Poincaré* **14**, 1927 (2013).
 - [12] A. Hatcher, Vector bundles and K-theory, 2003, <https://pi.math.cornell.edu/~hatcher/VBKT/VBpage.html> (2016).
 - [13] B. J. Wieder and B. A. Bernevig, The axion insulator as a pump of fragile topology, [arXiv:1810.02373](https://arxiv.org/abs/1810.02373).
 - [14] B. Bradlyn, Z. Wang, J. Cano, and B. A. Bernevig, Disconnected elementary band representations, fragile topology, and Wilson loops as topological indices: An example on the triangular lattice, *Phys. Rev. B* **99**, 045140 (2019).
 - [15] S. Liu, A. Vishwanath, and E. Khalaf, Shift Insulators: Rotation-Protected Two-Dimensional Topological Crystalline Insulators, *Phys. Rev. X* **9**, 031003 (2019).
 - [16] A. Bouhon, A. M. Black-Schaffer, and R.-J. Slager, Wilson loop approach to fragile topology of split elementary band representations and topological crystalline insulators with time-reversal symmetry, *Phys. Rev. B* **100**, 195135 (2019).
 - [17] J. Ahn, S. Park, and B.-J. Yang, Failure of Nielsen-Ninomiya Theorem and Fragile Topology in Two-Dimensional Systems with Space-Time Inversion Symmetry: Application to Twisted

- Bilayer Graphene at Magic Angle, *Phys. Rev. X* **9**, 021013 (2019).
- [18] S. H. Kooi, G. van Miert, and C. Ortix, Classification of crystalline insulators without symmetry indicators: Atomic and fragile topological phases in twofold rotation symmetric systems, *Phys. Rev. B* **100**, 115160 (2019).
- [19] H.-X. Wang, G.-Y. Guo, and J.-H. Jiang, Band topology in classical waves: Wilson-loop approach to topological numbers and fragile topology, *New J. Phys.* **21**, 093029 (2019).
- [20] M. B. de Paz, M. G. Vergniory, D. Bercioux, A. García-Etxarri, and B. Bradlyn, Engineering fragile topology in photonic crystals: Topological quantum chemistry of light, *Phys. Rev. Research* **1**, 032005(R) (2019).
- [21] Y. Hwang, J. Ahn, and B.-J. Yang, Fragile topology protected by inversion symmetry: Diagnosis, bulk-boundary correspondence, and Wilson loop, *Phys. Rev. B* **100**, 205126(R) (2019).
- [22] Z.-D. Song, L. Elcoro, and B. A. Bernevig, Twisted bulk-boundary correspondence of fragile topology, *Science* **367**, 794 (2020).
- [23] V. Peri, Z.-D. Song, M. Serra-Garcia, P. Engeler, R. Queiroz, X. Huang, W. Deng, Z. Liu, B. A. Bernevig, and S. D. Huber, Experimental characterization of fragile topology in an acoustic metamaterial, *Science* **367**, 797 (2020).
- [24] Z.-D. Song, L. Elcoro, Y.-F. Xu, N. Regnault, and B. A. Bernevig, Fragile Phases as Affine Monoids: Classification and Material Examples, *Phys. Rev. X* **10**, 031001 (2020).
- [25] A. Alexandradinata, J. Höller, C. Wang, H. Cheng, and L. Lu, Crystallographic splitting theorem for band representations and fragile topological photonic crystals, *Phys. Rev. B* **102**, 115117 (2020).
- [26] Z. Li, H.-C. Chan, and Y. Xiang, Fragile topology based helical edge states in two-dimensional moon-shaped photonic crystals, *Phys. Rev. B* **102**, 245149 (2020).
- [27] C. Shang, X. Zang, W. Gao, U. Schwingenschlögl, and A. Manchon, Second-order topological insulator and fragile topology in topological circuitry simulation, [arXiv:2009.09167](https://arxiv.org/abs/2009.09167).
- [28] C. S. Chiu, D.-S. Ma, Z.-D. Song, B. A. Bernevig, and A. A. Houck, Fragile topology in line-graph lattices with two, three, or four gapped flat bands, *Phys. Rev. Research* **2**, 043414 (2020).
- [29] C.-Y. Ji, Y. Zhang, Y. Liao, X. Zhou, J.-H. Jiang, B. Zou, and Y. Yao, Fragile topologically protected perfect reflection for acoustic waves, *Phys. Rev. Research* **2**, 013131 (2020).
- [30] J. L. Mañes, Fragile phonon topology on the honeycomb lattice with time-reversal symmetry, *Phys. Rev. B* **102**, 024307 (2020).
- [31] A. Bouhon, G. F. Lange, and R.-J. Slager, Topological correspondence between magnetic space group representations, *Phys. Rev. B* **103**, 245127 (2021).
- [32] A. Bouhon, T. Bzdušek, and R.-J. Slager, Geometric approach to fragile topology beyond symmetry indicators, *Phys. Rev. B* **102**, 115135 (2020).
- [33] B. J. Wieder, Z. Wang, J. Cano, X. Dai, L. M. Schoop, B. Bradlyn, and B. A. Bernevig, Strong and fragile topological Dirac semimetals with higher-order Fermi arcs, *Nat. Commun.* **11**, 627 (2020).
- [34] A. Skurativska, S. S. Tsirkin, F. D. Natterer, T. Neupert, and M. H. Fischer, Flat bands with fragile topology through superlattice engineering on single-layer graphene, *Phys. Rev. Research* **3**, 032003 (2021).
- [35] G. F. Lange, A. Bouhon, and R.-J. Slager, Subdimensional topologies, indicators and higher order phases, *Phys. Rev. B* **103**, 195145 (2021).
- [36] M. Koshino, N. F. Q. Yuan, T. Koretsune, M. Ochi, K. Kuroki, and L. Fu, Maximally Localized Wannier Orbitals and the Extended Hubbard Model for Twisted Bilayer Graphene, *Phys. Rev. X* **8**, 031087 (2018).
- [37] L. Zou, H. C. Po, A. Vishwanath, and T. Senthil, Band structure of twisted bilayer graphene: Emergent symmetries, commensurate approximants, and Wannier obstructions, *Phys. Rev. B* **98**, 085435 (2018).
- [38] J. Kang and O. Vafek, Symmetry, Maximally Localized Wannier States, and a Low-Energy Model for Twisted Bilayer Graphene Narrow Bands, *Phys. Rev. X* **8**, 031088 (2018).
- [39] J. Liu, J. Liu, and X. Dai, Pseudo Landau level representation of twisted bilayer graphene: Band topology and implications on the correlated insulating phase, *Phys. Rev. B* **99**, 155415 (2019).
- [40] H. C. Po, L. Zou, T. Senthil, and A. Vishwanath, Faithful tight-binding models and fragile topology of magic-angle bilayer graphene, *Phys. Rev. B* **99**, 195455 (2019).
- [41] Z. Song, Z. Wang, W. Shi, G. Li, C. Fang, and B. A. Bernevig, All Magic Angles in Twisted Bilayer Graphene Are Topological, *Phys. Rev. Lett.* **123**, 036401 (2019).
- [42] Z.-D. Song, B. Lian, N. Regnault, and A. B. Bernevig, TBG II: Stable symmetry anomaly in twisted bilayer graphene, *Phys. Rev. B* **103**, 205412 (2021).
- [43] J. Herzog-Arbeitman, Z.-D. Song, N. Regnault, and B. A. Bernevig, Hofstadter Topology: Noncrystalline Topological Materials at High Flux, *Phys. Rev. Lett.* **125**, 236804 (2020).
- [44] B. Lian, F. Xie, and B. A. Bernevig, Landau level of fragile topology, *Phys. Rev. B* **102**, 041402(R) (2020).
- [45] V. Peri, Z.-D. Song, B. A. Bernevig, and S. D. Huber, Fragile Topology and Flat-Band Superconductivity in the Strong-Coupling Regime, *Phys. Rev. Lett.* **126**, 027002(R) (2021).
- [46] Here, for boundary modes to be nontrivial, (i) their spectrum must be inside the bulk gap, and (ii) they are stable even when the underlying Hilbert space includes all irreducible symmetry representations.
- [47] L. E. Sadler, J. M. Higbie, S. R. Leslie, M. Vengalattore, and D. M. Stamper-Kurn, Spontaneous symmetry breaking in a quenched ferromagnetic spinor Bose–Einstein condensate, *Nature (London)* **443**, 312 (2006).
- [48] T. Oka and H. Aoki, Photovoltaic Hall effect in graphene, *Phys. Rev. B* **79**, 081406(R) (2009).
- [49] J.-i. Inoue and A. Tanaka, Photoinduced Transition Between Conventional and Topological Insulators in Two-Dimensional Electronic Systems, *Phys. Rev. Lett.* **105**, 017401(R) (2010).
- [50] T. Kitagawa, E. Berg, M. Rudner, and E. Demler, Topological characterization of periodically driven quantum systems, *Phys. Rev. B* **82**, 235114 (2010).
- [51] N. H. Lindner, G. Refael, and V. Galitski, Floquet topological insulator in semiconductor quantum wells, *Nat. Phys.* **7**, 490 (2011).
- [52] L. Jiang, T. Kitagawa, J. Alicea, A. R. Akhmerov, D. Pekker, G. Refael, J. I. Cirac, E. Demler, M. D. Lukin, and P. Zoller,

- Majorana Fermions in Equilibrium and in Driven Cold-Atom Quantum Wires, *Phys. Rev. Lett.* **106**, 220402 (2011).
- [53] T. Kitagawa, T. Oka, A. Brataas, L. Fu, and E. Demler, Transport properties of nonequilibrium systems under the application of light: Photoinduced quantum Hall insulators without Landau levels, *Phys. Rev. B* **84**, 235108 (2011).
- [54] B. Dóra, J. Cayssol, F. Simon, and R. Moessner, Optically Engineering the Topological Properties of a Spin Hall Insulator, *Phys. Rev. Lett.* **108**, 056602 (2012).
- [55] M. S. Rudner, N. H. Lindner, E. Berg, and M. Levin, Anomalous Edge States and the Bulk-Edge Correspondence for Periodically Driven Two-Dimensional Systems, *Phys. Rev. X* **3**, 031005 (2013).
- [56] M. Thakurathi, A. A. Patel, D. Sen, and A. Dutta, Floquet generation of Majorana end modes and topological invariants, *Phys. Rev. B* **88**, 155133 (2013).
- [57] Y. H. Wang, H. Steinberg, P. Jarillo-Herrero, and N. Gedik, Observation of Floquet-Bloch states on the surface of a topological insulator, *Science* **342**, 453 (2013).
- [58] J. Cayssol, B. Dóra, F. Simon, and R. Moessner, Floquet topological insulators, *Phys. Status Solidi RRL* **7**, 101 (2013).
- [59] M. C. Rechtsman, J. M. Zeuner, Y. Plotnik, Y. Lumer, D. Podolsky, F. Dreisow, S. Nolte, M. Segev, and A. Szameit, Photonic Floquet topological insulators, *Nature (London)* **496**, 196 (2013).
- [60] Z. Zhou, I. I. Satija, and E. Zhao, Floquet edge states in a harmonically driven integer quantum Hall system, *Phys. Rev. B* **90**, 205108 (2014).
- [61] M. Lababidi, I. I. Satija, and E. Zhao, Counter-Propagating Edge Modes and Topological Phases of a Kicked Quantum Hall System, *Phys. Rev. Lett.* **112**, 026805 (2014).
- [62] F. Nathan and M. S. Rudner, Topological singularities and the general classification of Floquet-Bloch systems, *New J. Phys.* **17**, 125014 (2015).
- [63] C. W. von Keyserlingk and S. L. Sondhi, Phase structure of one-dimensional interacting Floquet systems. I. Abelian symmetry-protected topological phases, *Phys. Rev. B* **93**, 245145 (2016).
- [64] Y.-G. Peng, C.-Z. Qin, D.-G. Zhao, Y.-X. Shen, X.-Y. Xu, M. Bao, H. Jia, and X.-F. Zhu, Experimental demonstration of anomalous Floquet topological insulator for sound, *Nat. Commun.* **7**, 13368 (2016).
- [65] D. V. Else and C. Nayak, Classification of topological phases in periodically driven interacting systems, *Phys. Rev. B* **93**, 201103(R) (2016).
- [66] E. Zhao, Anatomy of a periodically driven p-wave superconductor, *Z. Naturforschung Teil A* **71**, 883 (2016).
- [67] M. Fruchart, Complex classes of periodically driven topological lattice systems, *Phys. Rev. B* **93**, 115429 (2016).
- [68] I.-D. Potirniche, A. C. Potter, M. Schleier-Smith, A. Vishwanath, and N. Y. Yao, Floquet Symmetry-Protected Topological Phases in Cold-Atom Systems, *Phys. Rev. Lett.* **119**, 123601 (2017).
- [69] L. J. Maczewsky, J. M. Zeuner, S. Nolte, and A. Szameit, Observation of photonic anomalous Floquet topological insulators, *Nat. Commun.* **8**, 13756 (2017).
- [70] S. Mukherjee, A. Spracklen, M. Valiente, E. Andersson, P. Öhberg, N. Goldman, and R. R. Thomson, Experimental observation of anomalous topological edge modes in a slowly driven photonic lattice, *Nat. Commun.* **8**, 13918 (2017).
- [71] R. Roy and F. Harper, Periodic table for Floquet topological insulators, *Phys. Rev. B* **96**, 155118 (2017).
- [72] S. Yao, Z. Yan, and Z. Wang, Topological invariants of Floquet systems: General formulation, special properties, and Floquet topological defects, *Phys. Rev. B* **96**, 195303 (2017).
- [73] A. Eckardt, Colloquium: Atomic quantum gases in periodically driven optical lattices, *Rev. Mod. Phys.* **89**, 011004 (2017).
- [74] M. Tarnowski, F. N. Ünal, N. Fläschner, B. S. Rem, A. Eckardt, K. Sengstock, and C. Weitenberg, Measuring topology from dynamics by obtaining the Chern number from a linking number, *Nat. Commun.* **10**, 1728 (2019).
- [75] T. Oka and S. Kitamura, Floquet engineering of quantum materials, *Annu. Rev. Condens. Matter Phys.* **10**, 387 (2019).
- [76] M. S. Rudner and N. H. Lindner, Band structure engineering and non-equilibrium dynamics in Floquet topological insulators, *Nat. Rev. Phys.* **2**, 229 (2020).
- [77] M. Nakagawa, R.-J. Slager, S. Higashikawa, and T. Oka, Wannier representation of Floquet topological states, *Phys. Rev. B* **101**, 075108 (2020).
- [78] K. Wintersperger, C. Braun, F. N. Ünal, A. Eckardt, M. D. Liberto, N. Goldman, I. Bloch, and M. Aidelsburger, Realization of an anomalous Floquet topological system with ultracold atoms, *Nat. Phys.* **16**, 1058 (2020).
- [79] T. Morimoto, H. C. Po, and A. Vishwanath, Floquet topological phases protected by time glide symmetry, *Phys. Rev. B* **95**, 195155 (2017).
- [80] S. Xu and C. Wu, Space-Time Crystal and Space-Time Group, *Phys. Rev. Lett.* **120**, 096401 (2018).
- [81] S. Franca, J. van den Brink, and I. C. Fulga, An anomalous higher-order topological insulator, *Phys. Rev. B* **98**, 201114(R) (2018).
- [82] M. Rodríguez-Vega, A. Kumar, and B. Seradjeh, Higher-order Floquet topological phases with corner and bulk bound states, *Phys. Rev. B* **100**, 085138 (2019).
- [83] Y. Peng and G. Refael, Floquet Second-Order Topological Insulators from Nonsymmorphic Space-Time Symmetries, *Phys. Rev. Lett.* **123**, 016806 (2019).
- [84] K. Ladovrechis and I. C. Fulga, Anomalous Floquet topological crystalline insulators, *Phys. Rev. B* **99**, 195426 (2019).
- [85] R. Seshadri, A. Dutta, and D. Sen, Generating a second-order topological insulator with multiple corner states by periodic driving, *Phys. Rev. B* **100**, 115403 (2019).
- [86] K. Plekhanov, M. Thakurathi, D. Loss, and J. Klinovaja, Floquet second-order topological superconductor driven via ferromagnetic resonance, *Phys. Rev. Research* **1**, 032013(R) (2019).
- [87] T. Nag, V. Juričić, and B. Roy, Out of equilibrium higher-order topological insulator: Floquet engineering and quench dynamics, *Phys. Rev. Research* **1**, 032045(R) (2019).
- [88] R. W. Bomantara, L. Zhou, J. Pan, and J. Gong, Coupled-wire construction of static and Floquet second-order topological insulators, *Phys. Rev. B* **99**, 045441 (2019).
- [89] S. Chaudhary, A. Haim, Y. Peng, and G. Refael, Phonon-induced Floquet second-order topological phases protected by space-time symmetries, *Phys. Rev. Research* **2**, 043431 (2020).

- [90] A. K. Ghosh, G. C. Paul, and A. Saha, Higher order topological insulator via periodic driving, *Phys. Rev. B* **101**, 235403 (2020).
- [91] H. Hu, B. Huang, E. Zhao, and W. V. Liu, Dynamical Singularities of Floquet Higher-Order Topological Insulators, *Phys. Rev. Lett.* **124**, 057001 (2020).
- [92] B. Huang and W. V. Liu, Floquet Higher-Order Topological Insulators with Anomalous Dynamical Polarization, *Phys. Rev. Lett.* **124**, 216601 (2020).
- [93] R. W. Bomantara and J. Gong, Measurement-only quantum computation with Floquet Majorana corner modes, *Phys. Rev. B* **101**, 085401 (2020).
- [94] Y. Peng, Floquet higher-order topological insulators and superconductors with space-time symmetries, *Phys. Rev. Research* **2**, 013124 (2020).
- [95] R. W. Bomantara, Time-induced second-order topological superconductors, *Phys. Rev. Research* **2**, 033495 (2020).
- [96] T. Nag, V. Juricic, and B. Roy, Hierarchy of higher-order Floquet topological phases in three dimensions, *Phys. Rev. B* **103**, 115308 (2021).
- [97] A. K. Ghosh, T. Nag, and A. Saha, Floquet generation of second order topological superconductor, *Phys. Rev. B* **103**, 045424 (2021).
- [98] R.-X. Zhang and Z.-C. Yang, Tunable fragile topology in Floquet systems, *Phys. Rev. B* **103**, L121115 (2021).
- [99] W. Zhu, Y. D. Chong, and J. Gong, Floquet higher order topological insulator in a periodically driven bipartite lattice, *Phys. Rev. B* **103**, L041402 (2021).
- [100] R.-X. Zhang and Z.-C. Yang, Theory of anomalous Floquet higher-order topology: Classification, characterization, and bulk-boundary correspondence, [arXiv:2010.07945](https://arxiv.org/abs/2010.07945).
- [101] H. Chen and W. V. Liu, Intertwined space-time symmetry, orbital magnetism and dynamical Berry curvature in a circularly shaken optical lattice, *Phys. Rev. A* **104**, 013308 (2021).
- [102] W. Zhu, H. Xue, J. Gong, Y. Chong, and B. Zhang, Time-periodic corner states from Floquet higher-order topology, [arXiv:2012.08847](https://arxiv.org/abs/2012.08847).
- [103] J. Yu, R.-X. Zhang, and Z.-D. Song, Dynamical symmetry indicators for Floquet crystals, *Nat. Commun.* **12**, 5985 (2021).
- [104] W. Zhu, Y. Chong, and J. Gong, Symmetry analysis of anomalous Floquet topological phases, *Phys. Rev. B* **104**, L020302 (2021).
- [105] D. J. Thouless, M. Kohmoto, M. P. Nightingale, and M. den Nijs, Quantized Hall Conductance in a Two-Dimensional Periodic Potential, *Phys. Rev. Lett.* **49**, 405 (1982).
- [106] See Supplemental Material at <http://link.aps.org/supplemental/10.1103/PhysRevB.104.L180303> for the OTSL, the 2+1D example, and the 1+1D example.
- [107] F. D. M. Haldane, Model for a Quantum Hall Effect without Landau Levels: Condensed-Matter Realization of the “Parity Anomaly”, *Phys. Rev. Lett.* **61**, 2015 (1988).
- [108] C.-Z. Chang, J. Zhang, X. Feng, J. Shen, Z. Zhang, M. Guo, K. Li, Y. Ou, P. Wei, L.-L. Wang, Z.-Q. Ji, Y. Feng, S. Ji, X. Chen, J. Jia, X. Dai, Z. Fang, S.-C. Zhang, K. He, Y. Wang *et al.*, Experimental observation of the quantum anomalous Hall effect in a magnetic topological insulator, *Science* **340**, 167 (2013).
- [109] Y.-F. Zhao, R. Zhang, R. Mei, L.-J. Zhou, H. Yi, Y.-Q. Zhang, J. Yu, R. Xiao, K. Wang, N. Samarth *et al.*, Tuning the Chern number in quantum anomalous Hall insulators, *Nature (London)* **588**, 419 (2020).
- [110] C. Peng, A. Haim, T. Karzig, Y. Peng, and G. Refael, Floquet Majorana bound states in voltage-biased planar Josephson junctions, *Phys. Rev. Research* **3**, 023108 (2020).
- [111] R.-X. Zhang and S. D. Sarma, Anomalous Floquet Chiral Topological Superconductivity in a Topological Insulator Sandwich Structure, *Phys. Rev. Lett.* **127**, 067001 (2021).
- [112] T. Ozawa, H. M. Price, A. Amo, N. Goldman, M. Hafezi, L. Lu, M. C. Rechtsman, D. Schuster, J. Simon, O. Zilberberg, and I. Carusotto, Topological photonics, *Rev. Mod. Phys.* **91**, 015006 (2019).